Gas-Phase Fragmentation of the Ag^+–Phenylalanine Complex: Cation–π Interactions and Radical Cation Formation

Tamer Shoeib, Alwin Cunje, Alan C. Hopkinson, and K. W. Michael Siu
Department of Chemistry and Center for Research in Mass Spectrometry, York University, Toronto, Ontario, Canada

Collision-induced dissociation experiments on the Ag^+–phenylalanine complex using several collision energies were shown to yield ten different fragment ions. Unambiguous assignment of these fragment ions were made by careful analysis of deuterium labeling experiments. The losses of H_2O, CO, CO_2, and AgH were commonly observed; also encountered were the losses of H_2, Ag, and H. Deuterium labeling experiments and density functional calculations have been employed to probe fragmentation mechanisms that account for all experimental results. (J Am Soc Mass Spectrom 2002, 13, 408–416) © 2002 American Society for Mass Spectrometry

The interactions of metal ions with amino acids and peptides in the gas phase is a topic of much current interest [1–3]. Attempts have been made to further our understanding of complicated biological processes by modeling them using carefully planned gas-phase studies. In the absence of solvent, one may study the intrinsic modes of binding governing metal–amino acid complexes. Mass spectrometric experiments thus offer great potential for exploring the formation and reactivity of isolated cationic species.

Amino acid complexes of transition metal ions were first observed and studied using fast atom bombardment (FAB) [4, 5]. However, the limited solubility of metal salts and poor sensitivity prevented widespread systematic study of these complexes. Sensitivity is not typically an issue in matrix-assisted laser desorption/ionization (MALDI) [6, 7], but the fragmentation yields of its metastably decomposing ions are often poor. As the fragment ions potentially give information on atom connectivity and hence structure, MALDI is therefore non-ideal for examining fragmentation pathways. One technique that has proven effective for the study of metal-containing amino acids and peptides, and the one employed here, is electrospray tandem mass spectrometry. First, electrospray ionization [8] is a soft ionization method and one that is efficient at producing gas-phase metal-containing ions [9–15], whose solubility in water or water/methanol is typically high. Second, fragmentation is efficient and is easily controlled via collision-induced dissociation, the energy of which is crucial in directing fragmentation products and their yield.

Molecular orbital calculations are frequently combined with experiments in studies to obtain a better understanding of the structure and thermochemistry of the organometallic species of interest [1, 2, 16, 17]. Recent density functional molecular orbital studies have shown that Ag^+ can be mono-, di-, or tricoordinate in complexes with α-amino acids [18]; tetracoordinate Ag^+ has been postulated for relatively small peptides [19, 20]. The binding of silver(I) to glycine, diglycine, and triglycine, and to a number of other polypeptides, has been investigated [19, 20]. In particular, the structures of argentinated glycine and its oligomers have been examined in detail by means of density functional theory [21].

The focus of this paper is the Ag^+–phenylalanine complex. Theory has shown the binding energy of Ag^+ to phenylalanine to be about 7 kcal mol^{-1} higher than that of Ag^+ to glycine [18]. This suggests that the interactions of Ag^+ with the π-system is present in the lowest energy conformer of the Ag^+–phenylalanine complex. π Interactions with metal cations are noncovalent and have been suggested as being important in molecular recognition by biological receptors, in enzyme catalysis and in the design of novel ionophores. One of the objectives of this study is to provide some experimental evidence of Ag^+–π interactions in phenylalanine as a test system for other aromatic amino acids. A survey of the collision-induced dissociation products of the Ag^+–phenylalanine complex is provided and

Published online March 1, 2002
Address reprint requests to Dr. K. W. M. Siu, Department of Chemistry and Center for Research in Mass Spectrometry, York University, 4700 Keele Street, Toronto, Ontario M3J 1P3, Canada. E-mail: kwmsiu@yorku.ca

1044-0305/02/$20.00
PII S1044-0305(02)00353-7

Received July 23, 2001
Revised January 9, 2002
Accepted January 9, 2002

mechanisms for the dissociation reactions are postulated. These are supported by the results of deuterium-labeling experiments and by density functional theory (DFT) calculations.

Experimental

Materials

Stock solutions were prepared by separately dissolving 2–3 mg of phenylalanine (99% Aldrich 14,796-6) and 2–3 mg of $AgNO_3$ (99.8% Sigma S-0139) each in 1 mL of H_2O. Sample solutions were typically 1 mM in phenylalanine and 0.1 mM in $AgNO_3$ in a mixture of 1:1 (vol/vol) H_2O/CH_3OH. Deionized water and reagent grade methanol (Aldrich) were used as solvents. Deuterium exchange experiments were carried out in solutions that contain deuterium oxide (99.9% D CDN isotopes) and CH_3OD (99.5% D Aldrich 15,193-9) instead of water and methanol.

Mass Spectrometry

Experiments were performed on an API 3000 prototype and an API III; both are AB SCIEX (Concord, Ontario) triple-quadrupole mass spectrometers. Sample solutions were continuously infused at a rate of 4 μL min^{-1} into the pneumatically-assisted electrospray probe using dry air as the nebulizer gas. Mass spectra were obtained in the positive ion detection mode with unit mass resolution, with a step size of 0.1 *m/z* unit and with a dwell time of 10 ms/step. Typically 10 scans were summed to produce a mass spectrum. Product and precursor ion spectra were obtained using nitrogen (argon in the case of the API III) as the collision gas at a pressure of about 3 mTorr. For the acquisition of product ion spectra center-of-mass collision energies (E_{cm}) in the range of 0.5–5 eV were employed; for precursor ion spectra laboratory collision energies (E_{lab}) between 5 and 50 eV were typically used. All precursor ion spectra discussed in this paper are available as supplementary material.

Computational Methods

Molecular orbital calculations were performed using Gaussian 98 [22]. All structures were optimized without symmetry constraints by density functional theory (DFT) using the B3LYP hybrid method [23–28]; the 6-311++G(d,p) basis set was used to examine the protonated phenylalanine complex, while the DZVP basis set [29, 30] was employed to study the Ag^+–phenylalanine complex and its collision-induced dissociation products. All critical points were characterized by harmonic frequency calculations and were shown to be at minima, unless otherwise stated. The B3LYP/DZVP level of theory was previously used to calculate enthalpies and free energies for association reactions of Ag^+ and a variety of ligands containing nitrogen [16, 31] and oxygen [32] donor atoms to within 2 kcal mol^{-1} of the experimental values. This level of theory was also successfully used to obtain silver ion affinities and basicities of all naturally-occurring amino acids [18]. These calculated basicities were shown to compare favorably with those obtained by the kinetic method [33]. The B3LYP/DZVP approach was also used to probe the fragmentation pathways and reaction mechanisms of silver-containing amines [34] and the Ag^+-proline complex in the gas phase [17].

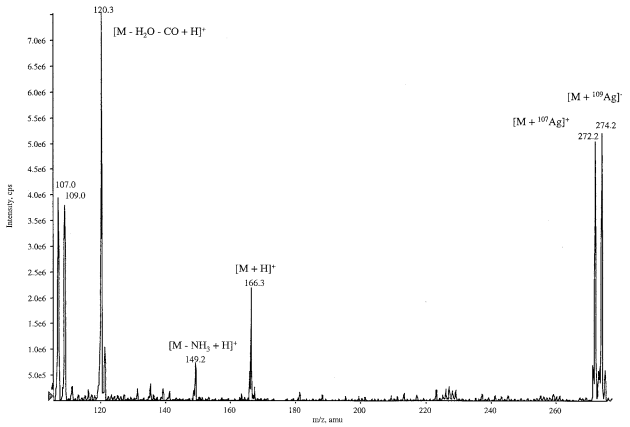

Figure 1. Positive ion mode electrospray mass spectrum of a solution of 1 mM phenylalanine and 0.1 mM $AgNO_3$ in 1:1 (vol/vol) H_2O/CH_3OH.

Results and Discussion

Electrospraying phenylalanine in the presence of Ag^+ produced an abundance of phenylalanine-containing ions (Figure 1), Ag^+–phenylalanine ions (*m/z* 272 and 274, corresponding to $[M + {}^{107}Ag]^+$ and $[M + {}^{109}Ag]^+$ {M = phenylalanine}, respectively). Peaks at *m/z* 107 and 109 are almost equally abundant; these correspond to the two isotopes of silver. Protonated phenylalanine ions (*m/z* 166) were also observed. A signal at *m/z* 149, due to the loss of NH_3 from protonated phenylalanine as a result of in-source fragmentation, was also evident. Ions at *m/z* 120, most likely corresponding to the loss of H_2O and CO from protonated phenylalanine, due to in-source fragmentation, provided the most abundant signal.

The fragmentation pattern of protonated phenylalanine is illustrated in Figure 2. A plausible reaction mechanism accounting for this fragmentation pattern is shown in Scheme **1**. The formation of an immonium ion (at *m/z* 120 in Figure 2), via the loss of 46 Th corresponding to the elements HCOOH has been commonly observed in the fragmentation of protonated amino acids and their complexes with Ni^+, Cu^+, Co^+ and Ag^+, and Zn^{2+} [1, 35–41]. It is the current consensus that the elements of HCOOH are not lost as a dihydroxycarbene, but rather as H_2O and CO. In the case of protonated phenylalanine this process produces the most abundant species, in agreement with Figure 1. Other

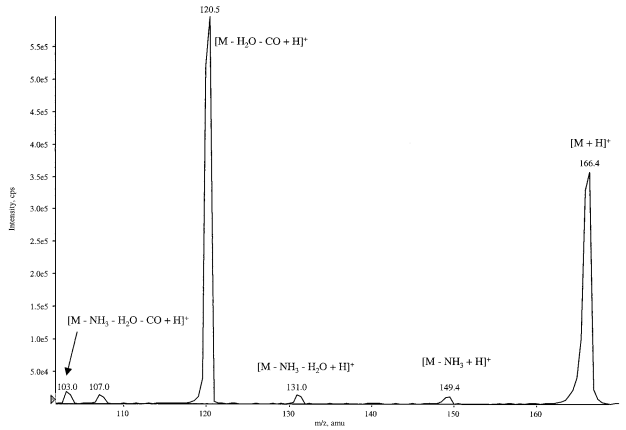

Figure 2. Collision-induced dissociation of protonated phenylalanine at 20.8 eV laboratory collision energy.

ions in the CID spectra of protonated phenylalanine such as those at *m/z* 149 corresponding to the loss of NH_3, at *m/z* 131 corresponding to the loss of NH_3 and H_2O, and those at *m/z* 103 corresponding to the loss of NH_3, H_2O, and CO, are all minor species. This indicates that the pathway to produce the immonium ion at *m/z* 120 is the most favorable. It has been suggested that the loss of NH_3 from protonated phenylalanine is facilitated by a phenyl group migration (Scheme **1**, Path B) to produce a phenonium ion, [36] which was shown to be stabilized by electron-donating groups such as an OH substituent in the para position in the case of tyrosine [35]. However, based on the relative energies of the products, the loss of NH_3 from protonated phenylalanine via a hydride-assisted migration (Scheme **1**, Path A) and the production of a benzyl cation, **1B** (see Figure 3) is calculated to be more favorable by 14.1 kcal mol^{-1} with respect to **1P**, the phenonium ion (see Scheme **1** and Figure 3). However, when reaction barriers for both processes are considered, the hydride migration was found to have a significant forward activation barrier, **1H** $\rightarrow$ **1B**, of 36.5 kcal mol^{-1}, while the phenyl migration proceeds without a barrier and thus only has to overcome the reaction's endoergicity. The phenyl migration process requires the phenyl ring and the $-NH_3^+$ group to be on opposite sides to allow for the production of the phenonium ion (see Figure 3). This conformation of the protonated phenylalanine complex, **1Ha**, is higher in free energy than **1H**, the conformation required for the hydride shift and the production of the benzyl cation by 6.6 kcal mol^{-1}. The interconversion pathway between the phenonium ion, **1P**, and the more thermodynamically stable benzyl ion, **1B**, was also considered and was found to proceed via transition state **1B** $\rightarrow$ **1P** which is 23.9 kcal mol^{-1} above the phenonium ion, **1P**; interconversion between the two ions is therefore unlikely. According to our optimizations at the B3LYP/6-31++G(d,p) level of theory, the tropylium ion was found to be 3.9 kcal mol^{-1} lower in energy than the benzyl cation and 17.7 kcal mol^{-1} lower than the phenonium ion. However, the pathway to interconversion between these ions was shown to have a high reaction barrier [42]. This lends further support to Harrison and co-workers' [36] suggestion that the loss of NH_3 from protonated phenylalanine proceeds by means of a phenyl migration. The phenonium ion does not subsequently rearrange to a thermodynamically more stable species, but instead loses H_2O to produce an ion at *m/z* 131, which in turn loses CO to produce the ion at *m/z* 103 as observed in Figure 2. The fact that the immonium ion (*m/z* 120), generated via the loss of H_2O and CO from protonated phenylalanine, is the most dominant species suggests that if Path C in Scheme **1** has a reaction barrier it must be significantly lower than 24.9 kcal mol^{-1}, which is the endoergicity required to generate the phenonium ion, **1P** (at *m/z* 149), while Path A may be discounted because of its relatively high reaction barrier.

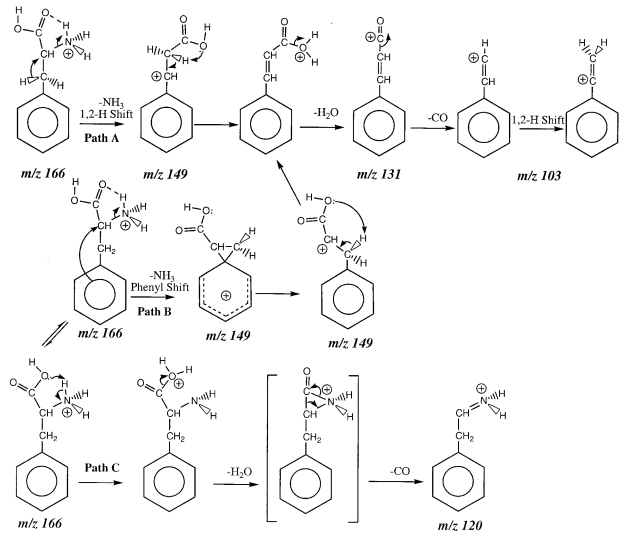

Scheme 1. Bold numbers are structure numbers; bold italicized numbers are nominal *m/z* values of ^{107}Ag- and ^{1}H-containing ions.

The fragmentation pattern of Ag^+–phenylalanine is given in Figure 4. Unambiguous assignment of the peaks can be made by comparing the product ion spectra of phenylalanine and that of d_3–phenylalanine (phenylalanine with its $-NH_2$ and COOH hydrogen atoms replaced by deuterium atoms) complexed with the two silver isotopes. Comparing the fragmentation patterns in Figure 4a and b, it is clear that each of the ions in these spectra contains silver with the exception of the ions at *m/z* 164, 146, 120, 119, and 118. The ions containing silver were assigned as $[M - H_2O + Ag]^+$ *m/z* 254 (Figure 4a), *m/z* 256 (Figure 4b); $[M - NH_3 - CO + Ag]^+$ *m/z* 227 (Figure 4a), *m/z* 229 (Figure 4b); $[M - H_2O - CO + Ag]^+$ *m/z* 226 (Figure 4a), *m/z* 228 (Figure 4b); $[M - NH_3 - CO_2 + Ag]^+$ *m/z* 211 (Figure 4a), *m/z* 213 (Figure 4b); $[Ag + NH_3]^+$ *m/z* 124 (Figure 4a), *m/z* 126 (Figure 4b); and Ag^+ *m/z* 107 (Figure 4a) *m/z* 109 (Figure 4b). The ions which do not contain silver, *m/z* 164 (Figure 4a and b), *m/z* 146 (Figure 4a and b) *m/z* 120 (Figure 4a and b), *m/z* 119 (Figure 4a and b) and *m/z* 118 (Figure 4a and b) are assigned as $[(M + Ag) - AgH]^+$, $[(M + Ag) - Ag - H_2O]^+$, $[(M + Ag) - AgH -$

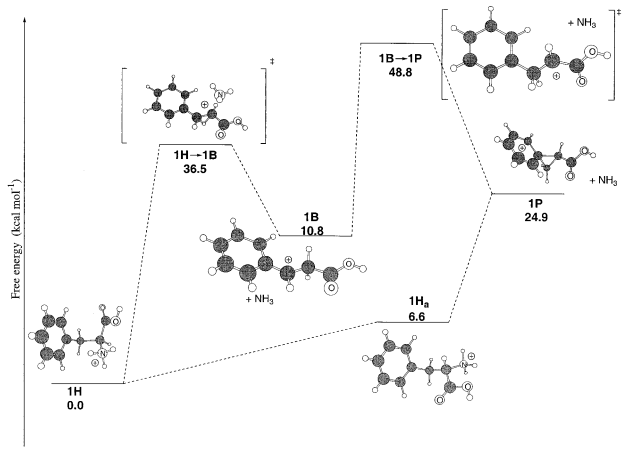

Figure 3. Relative free energies for species involved in the loss of NH_3 from protonated phenylalanine.

$CO_2]^+$, $[(M + Ag) - H_2O - CO - Ag]^+$ and $[(M + Ag) - H_2O - AgH - CO]^+$, respectively. A comparison of Figure 4b and c provides information on the number of labile (exchangeable) hydrogen atoms contained within the product ions. From this comparison it is apparent that the ions in Figure 4b at *m/z* 229 and 213 must contain no exchangeable hydrogen atoms, those at *m/z* 256, 228, and 146 must contain one exchangeable hydrogen atom, that at *m/z* 120 must contain two exchangeable hydrogen atoms and finally those at *m/z* 274, 164, and 126 must contain three exchangeable hydrogen atoms.

Some of the fragmentation products of Ag^+–phenylalanine observed in Figure 4 are analogous to fragments observed for amino acids cationized by a proton or by metal ions such as Cu^+, Fe^+ and Ni^+, [36–38, 40, 42, 43] while many of these fragment products in Figure 4 appear to be unique and may be induced by the presence of Ag^+ [41]. The loss of H_2O from Ag^+–phenylalanine was observed in the analogous Cu^+ complex [40]. The formation of an immonium ion via the loss of H_2O and CO observed in the CID of Ag^+–phenylalanine was also observed for most α-amino acid complexes with Ag^+ [44]. This fragmentation to yield an immonium ion is very common and has been observed for Cu^+ and Ni^+ complexes of phenylalanine [37, 38, 40], for the Zn^{2+} complex with glycine [39], and for protonated amino acids [36, 43] including phenylalanine, as is shown here in Figure 2.

By contrast, the CID spectra of K^+ and Cs^+ complexes with phenylalanine are reported to contain only the bare metal cation [41]. This is perhaps due to a lower binding affinity of phenylalanine to K^+ and Cs^+, compared to its binding affinity to Fe^+, Cu^+, Ni^+, or Ag^+. A higher binding affinity in the latter cases makes the metal ion dissociation pathway competitive with other dissociation pathways and thus product ions other than the bare metal ions are formed for these complexes. In fact, the CID spectrum of Ag^+–glycine is the only example in which the bare metal cation is the lone fragment observed [44]; theoretical calculations have shown that the binding energy of Ag^+ to glycine to be at least 2 kcal mol^{-1} lower than that of any other amino acid. Two pathways that appear to be unique to silver-cationized species are the loss of AgH and the formation of Ag^+–NH_3. The loss of AgH was previously observed in the CID of silver-cationized amines [34], as a product of the reaction of Ag^+ with hydrocarbons [45], and as a fragment product of Ag^+ complexes with most α-amino acids [44], including the Ag^+–proline complex [17]. The mechanism leading to the loss of a neutral AgH molecule was investigated in detail [17, 34].

Previous to these mechanistic studies, an alternate explanation based on C–H bond activation and metal insertion was proposed, but barriers for these processes were not obtained [45]. The formation of Ag^+–NH_3 requires the attachment of Ag^+ to a ligand containing at least one amino group and another coordination site. It is thus not surprising that this ion was not observed in the CID spectra of silver-cationized mono-amines [34], but was present in those of silver-cationized diamines (unpublished results). This ion is also a common fragmentation product of most of α-amino acid complexes with Ag^+ [44].

From the precursor ion spectrum of *m/z* 211 (provided in the Appendix), it is evident that the major source of this ion is the $[M + {}^{107}Ag]^+$ complex. Parenthetically, two peaks at *m/z* 243 and *m/z* 229 are observed and assigned as methanol and water adducts of the ion at *m/z* 211, due to the in-source fragmentation of $[M + {}^{107}Ag]^+$ to produce *m/z* 211 and its subsequent in-source complexation with the solvent molecules. These ions at *m/z* 243 and 229, in turn, lose CH_3OH and H_2O respectively to produce *m/z* 211, and are thus recorded in the precursor ion spectrum.

The precursor ion spectrum of *m/z* 164 (provided in the Appendix) shows the dominant source of these ions to be the ions $[M + Ag]^+$, with minor sources from ions at *m/z* 196 and 182, assigned as the adducts of *m/z* 164 with CH_3OH and H_2O, respectively. These adducts are most likely produced in the front-end of the mass spectrometer as previously described. These observations corroborate the formation of methanol and water adduct species to fragment ions of the Ag^+–phenylalanine complex most recently reported [41, 46].

The precursor ion spectrum of *m/z* 146 (provided in the Appendix) shows both $[M + Ag]^+$ and $[M - H_2O + Ag]^+$ ions as sources for *m/z* 146, while the precursor ion spectrum of *m/z* 124 (provided in the Appendix), assigned as $^{107}Ag^+$–NH_3, shows $[M + {}^{107}Ag]^+$ as its only source. The precursor ion spectrum of *m/z* 119 (provided in the Appendix) indicates *m/z* 120 as a major source. Protonated phenylalanine (*m/z* 166) is also shown as a source of *m/z* 119, which is most likely formed after concomitant loss of H_2O and CO from $[M + H]^+$ (see Figure 2 and Scheme **1**) to produce *m/z* 120, which subsequently loses $H^{\cdot}$ to produce *m/z* 119. The ions $[M + Ag]^+$ (*m/z* 272 and

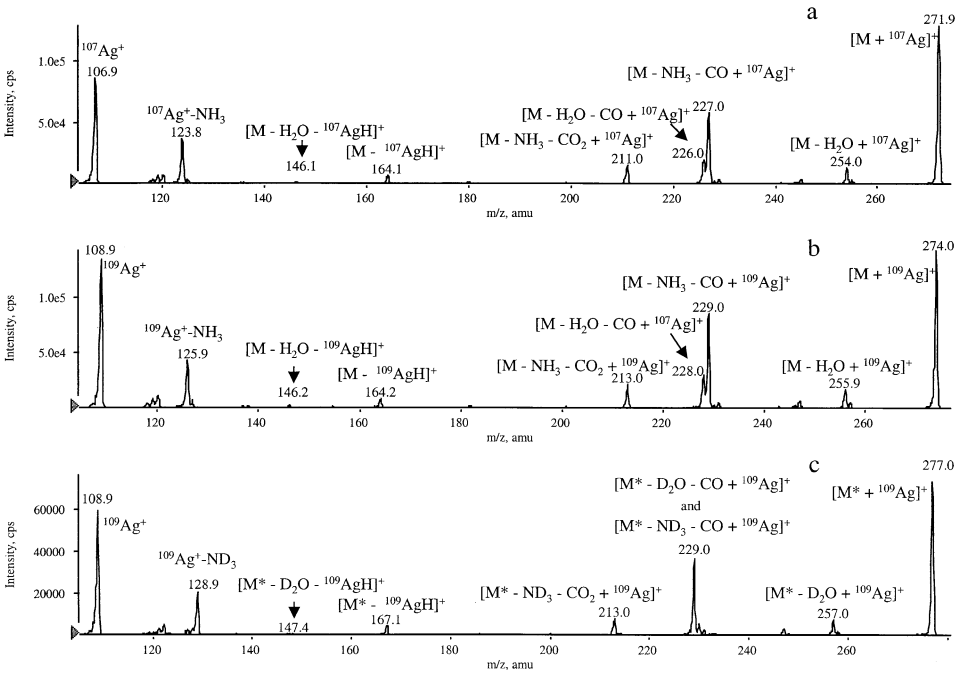

Figure 4. Collision-induced dissociation at 26.9 eV laboratory collision energy of (**a**) $^{107}Ag^+$–phenylalanine, (**b**) $^{109}Ag^+$–phenylalanine and (**c**) $^{109}Ag^+$-d_3–phenylalanine.

274) and $[M - H_2O - CO + Ag]^+$ (*m/z* 226 and 228) are relatively minor sources of *m/z* 119.

The precursor ion spectrum of *m/z* 118 (provided in the Appendix) shows the loss of H· from the ion at *m/z* 119 to be a dominant pathway of formation; a second prominent source is the ion at *m/z* 120. A minor source are the ions $[M - H_2O - CO + Ag]^+$ at *m/z* 226 and 228, which produce *m/z* 118 via neutral AgH loss, as is shown in Scheme **2**. The $[M + Ag]^+$ ions (*m/z* 272 and 274) are also a source for *m/z* 118. Taken collectively, the results strongly suggest that $[M + Ag]^+$ dissociates first to give $[M - H_2O - CO + Ag]^+$, which then dissociates to yield *m/z* 118 after the loss of AgH (Scheme **2**).

The structure at the global minimum on the Ag^+–phenylalanine complex surface is shown below (Structure **1**, see also Scheme **2**). In this form of the complex the silver ion is tricoordinate, binding to the carbonyl oxygen, the amino nitrogen and also interacting with the π-system of the phenyl ring of phenylalanine.

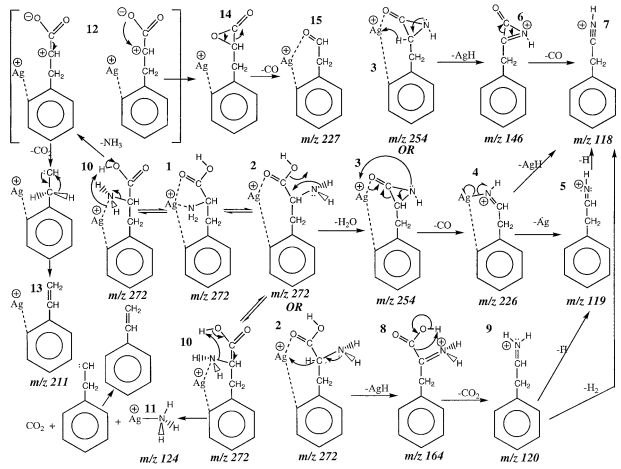

Scheme 2. Bold numbers are structure numbers; bold italicized numbers are nominal *m/z* values of ^{107}Ag- and ^1H-containing ions.

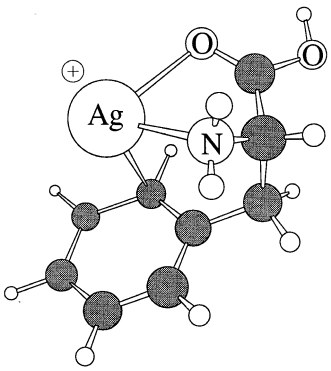

Structure 1

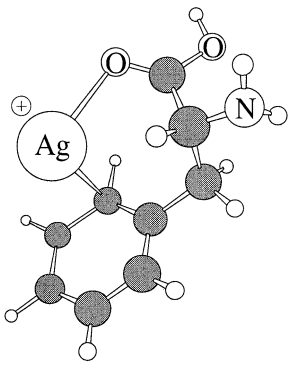

Structure 2

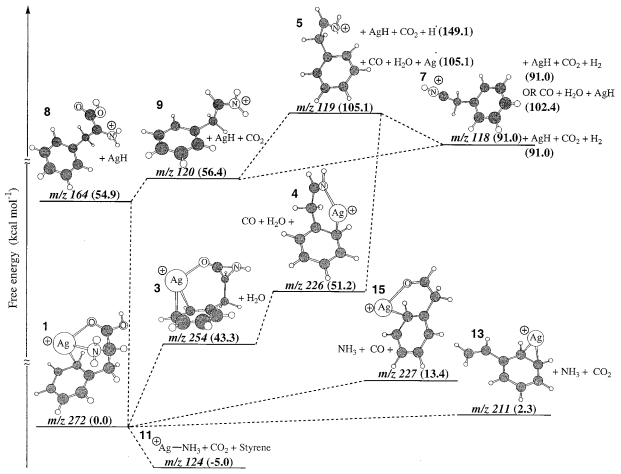

Figure 5. Relative free energies in parentheses at 298K in kcal mol^{-1} of Ag^+–phenylalanine and its dissociation products as calculated at B3LYP/DZVP. All structures are at minima. Italicized numbers are *m/z* values, bold numbers are structure numbers from Scheme **2**. The loss of Ag^+ from **1**, a common occurrence for other Ag^+-containing ions, is not included as the primary interest here is the fragmentation of the ligand.

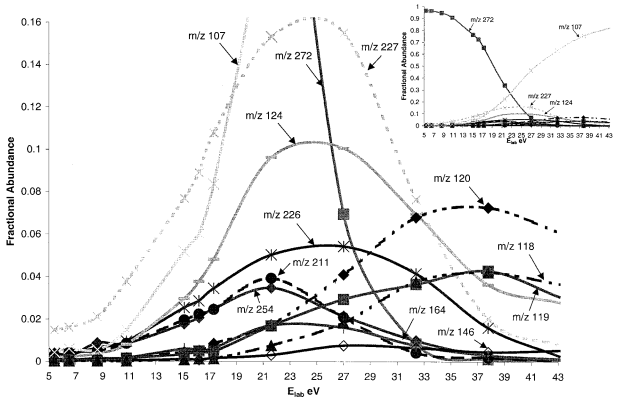

Figure 6. Energy-resolved collision-induced dissociation of $^{107}Ag^+$–phenylalanine. The full-scale figure in the top right hand corner is expanded and shown in the main figure for clarity.

The major difference between Structure **2** (see also Scheme **2**) and **1** is the absence of the Ag–N interaction; rearrangement of **1** leads to **2** by cleavage of one coordination bond. Structure **2** then loses H_2O (or D_2O for the d_3 analogue, see Scheme **2**) to produce **3**, an aziridinone structure which contains silver (see Figure 4a and b) and one labile (exchangeable) hydrogen atom in accordance with a shift from *m/z* 256 (Figure 4b) to *m/z* 257 (Figure 4c). This process from **1** to **3** has a reaction enthalpy and a free energy of 55.8 and 43.3 kcal mol^{-1}. Fragmentation of ion **1** is unusual in this regard as most argentinated amino acids lose both H_2O and CO simultaneously. Ion **3** subsequently loses CO producing **4**, a structure containing silver (see Figure 4a and b) and one labile hydrogen atom, in accordance with a shift from *m/z* 228 (Figure 4b) to *m/z* 229 (Figure 4c). This reaction from **3** to **4** has enthalpy and free energy changes of 18.7 and 7.8 kcal mol^{-1}, respectively. Structure **4** in turn loses a silver atom to produce **5**, a radical cation with a *m/z* of 119, containing only one exchangeable hydrogen atom. This is consistent with the spectra in Figure 4 and the previously discussed precursor ion scan results. The reaction enthalpy and free energy for conversion of **4** to **5** are 82.8 and 54.0 kcal mol^{-1}, respectively. Structure **4** also loses AgH via a different pathway to produce **7**, having a *m/z* 118 and containing one exchangeable hydrogen atom (Scheme **2**). Conversion of **4** to **7** has a reaction enthalpy of 81.5 and a free energy of 70.3 kcal mol^{-1}.

The aziridinone, Structure **3**, also loses AgH to produce **6**, an ion which does not contain silver but has one exchangeable hydrogen atom (Scheme **2**), in accordance with the results of product ion scans (Figure 4) and precursor ion scans (Appendix). Ion **6** subsequently loses CO to produce **7**.

From Structure **2** the loss of AgH produces **8**, an ion containing three exchangeable hydrogen atoms, in accordance with the shift from *m/z* 164 (Figure 4a and b) to *m/z* 167 (Figure 4c). The enthalpy for conversion from **1** to **8** is 66.5 and the free energy 54.9 kcal mol^{-1}. Subsequent loss of CO_2 from **8** produces **9**, an ion with a *m/z* value of 120 (see Figure 4). This reaction has an enthalpy of 12.4 and a free energy of 1.5 kcal mol^{-1}. Structure **9** subsequently loses either a hydrogen atom to produce **5** or a hydrogen molecule to produce **7**, in accordance with precursor ion scan data.

Structure **10** is yet another form of the $[M + Ag]^+$ complex and is in equilibrium with **1** and **2**. The loss of CO_2 and styrene from **10** produces Ag^+–NH_3 or Ag^+–ND_3, ion **11**. From Figure 4a and b it is clear that **11** contains silver and the shift from *m/z* 126 (Figure 4b) to *m/z* 129 (Figure 4c) indicates the presence of three exchangeable hydrogen atoms. Precursor ion scans indicate that the $[M + Ag]^+$ ions are the only precursors to Ag^+–NH_3. The enthalpy for converting **1** to **11** is 19.7 and the free energy −5.0 kcal mol^{-1}.

Structure **10** can also lose NH_3 (or ND_3 for the d_3 analogue) to produce a transient zwitterionic species, **12**, which loses CO_2 to produce a carbene that, in turn, rearranges to **13**, a styrene molecule with Ag^+ complexed to the π-system of the phenyl ring. Structure **13** contains a silver atom, in accordance with the shift from *m/z* 211 (Figure 4a) to *m/z* 213 (Figure 4b) and contains no exchangeable hydrogen atoms, in accordance with Figure 4b and c. Precursor ion data (shown in the Appendix) show that the $[M + Ag]^+$ ions are the predominant source of the *m/z* 211 ion. The reaction enthalpy from **1** to **13** is 27.5 and the free energy 2.3 kcal mol^{-1}.

The zwitterion **12** could also rearrange to an aziridinone structure **14**, which subsequently loses CO to produce **15**, a structure containing silver, in accordance with the shift from *m/z* 227 (Figure 4a) to *m/z* 229 (Figure 4b) and contains no exchangeable hydrogen atoms, in accordance with the peak at *m/z* 229 (Figure 4c). The

enthalpy for conversion of **1** to **15** is 37.6 and the free energy 13.4 kcal mol^{-1}.

The structures of the ions observed and their relative free energies as calculated at B3LYP/DZVP are presented in Figure 5. This figure shows that the fragment ions can be classified into three energy groups. The first group is composed of the ions at *m/z* 124, 211, and 227. These ions all have reaction free energies lower than 15 kcal mol^{-1}. The second group is composed of the ions at *m/z* 254, 226, 164, and 120. This latter group of ions have reaction free energies between 40 and 60 kcal mol^{-1}. A final group of ions are those at *m/z* 118 and 119. These two ions have a substantially higher reaction free energies at 91 and 105 kcal mol^{-1}, respectively. It is interesting to note that the summed free energy of formation for the radical cation, **5**, observed at *m/z* 119, and its fragmentation partners AgH, CO_2 and H (if ion, **10**, at *m/z* 120 is its precursor) or CO, H_2O and Ag (if ion, **4**, at *m/z* 226 is its precursor), i.e., the reaction free energy is the highest among all species observed relative to **1**. These calculated free energies are the minimum values for the reaction barriers. Bearing in mind that the collision-induced dissociations were carried out under conditions in which there were tens of collisions, ions that were observed under low lab-energy conditions must, therefore, have relatively low calculated free energies of dissociation. The reverse, however, is not necessarily true, as an ion that has a low free energy relative to **1** may require significant rearrangement to allow its formation, and thus have a high reaction barrier.

The variation of fragmentation abundances as a function of collision energy is shown in Figure 6. From these energy-resolved CID experiments it is apparent that the loss of $^{107}Ag^+$ from $[M + {}^{107}Ag]^+$, loss of NH_3 and CO_2 from $[M + {}^{107}Ag]^+$ to form $^{107}Ag^+$–styrene, ion **13**, at *m/z* 211, loss of H_2O from $[M + {}^{107}Ag]^+$ to form the aziridinone, ion **3**, at *m/z* 254, and loss of ^{107}AgH from $[M + {}^{107}Ag]^+$ to form $[M - {}^{107}Ag]^+$, ion **8**, at *m/z* 164 are efficient processes at relatively low lab-energy collision conditions. At slightly higher collision energy conditions the formation of ions **15**, **11**, and **4** at *m/z* 227, 124, and 226, respectively, become dominant pathways. It is interesting that while Figure 5 shows the formation of ion **11** (*m/z* 124) from **1** to be exoergic by 5 kcal mol^{-1}, based on the summed free energies of Ag^+–NH_3, ion **11**, CO_2 and styrene relative to $[M + Ag]^+$, ion **1**, the energy-resolved CID spectrum in Figure 6 shows that this reaction is not spontaneous, and that ion **11** reaches its maximum fractional abundance at a lab-energy of about 25 eV. This clearly indicates that this process must have a barrier consistent with some major rearrangement as proposed in Scheme **2**. Figure 6 also shows that the formation of the ions **9**, **5**, and **7** at *m/z* 120, 119, and 118, respectively, become significant pathways only at very high lab energies, reaching their maximum fractional abundance at about 38 eV in the lab frame. All of these ions were calculated to have relatively high reaction free energies and possibly even higher activation barriers (see Figure 5).

Silver-containing ions, with the exception of **11**, have Ag^+–π interactions with the phenyl ring. The loss of silver atom observed here produces a radical cation **5**, which together with the neutral products yields the highest relative free energy. In the fragmentation of Ag^+ complexes of amino acids that contain aliphatic side chains, the losses of H_2O and CO are concomitant; however, in the case of Ag^+–phenylalanine, the ion produced by the loss of only water, **3**, is not only observed, but is one of the dominant ions at low lab energies. The stability of this ion is attributed to Ag^+–π interaction with the phenyl ring. After the submission of this contribution, a paper by Perera et al. [46] appeared in which most of the observations and conclusions independently reported here are corroborated. We thank one of the reviewers for pointing out possible alternative pathways for the fragmentation reactions observed for the Ag^+–phenylalanine complex that involve activation of and insertion of the metal ion into various C–C, C–N, and C–H bonds and eventual fragmentation, which have previously been suggested for Cu^+–phenylalanine [40, 47] and for Ag^+–hydrocarbon complexes [45]. These pathways appear to be high-energy processes; ruling them out, however, would require a substantial amount of work and is best left to a future investigation.

Acknowledgments

The authors are grateful to the reviewers of this manuscript for their very insightful and helpful suggestions, and to Houssain El Aribi and Steve Quan for technical assistance. The authors thank the Natural Sciences and Engineering Council of Canada (NSERC), MDS SCIEX, the Canadian Foundation for Innovation (CFI), and the Ontario Innovation Trust (OIT) for financial support. TS acknowledges financial support in the form of an Ontario Graduate Scholarship in Science and Technology.

Appendix

Precursor ion scans for *m/z* 211, 164, 146, 124, 119, and 118 are shown.

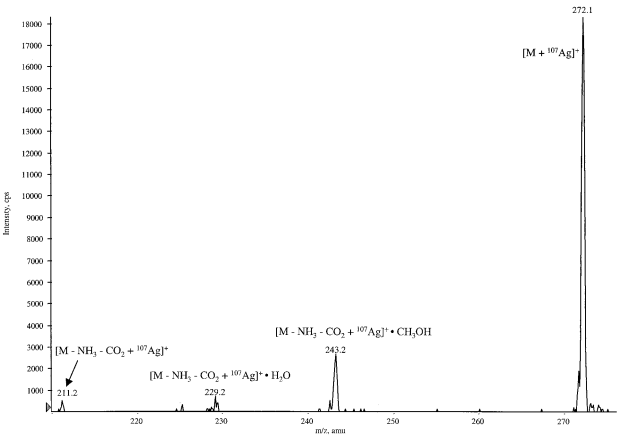

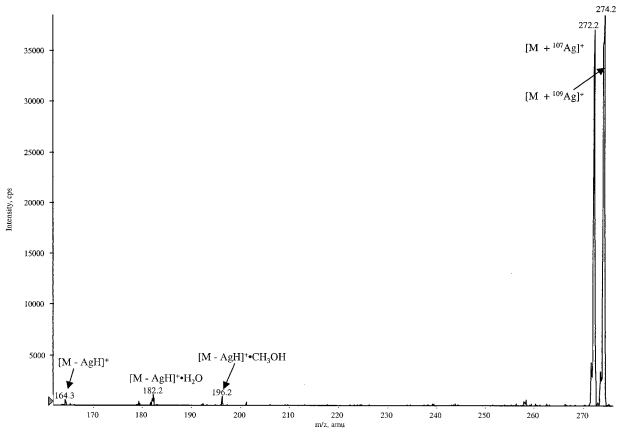

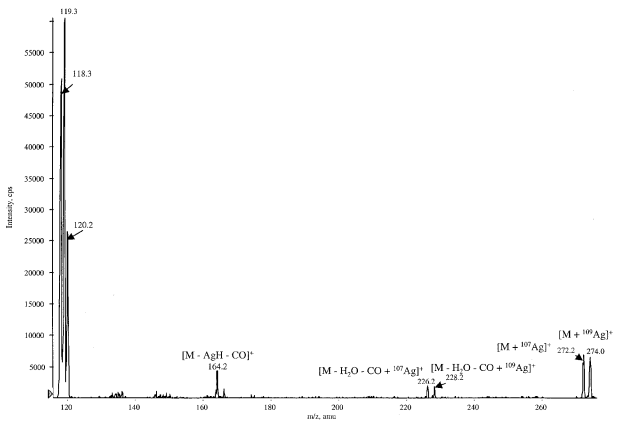

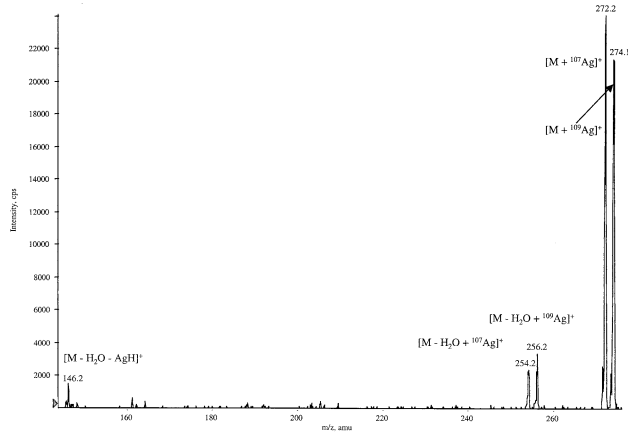

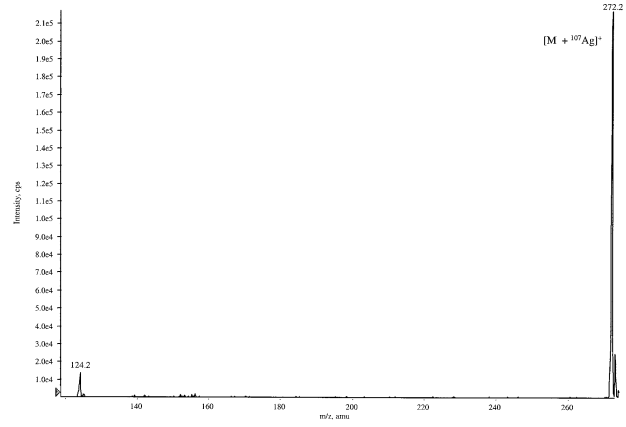

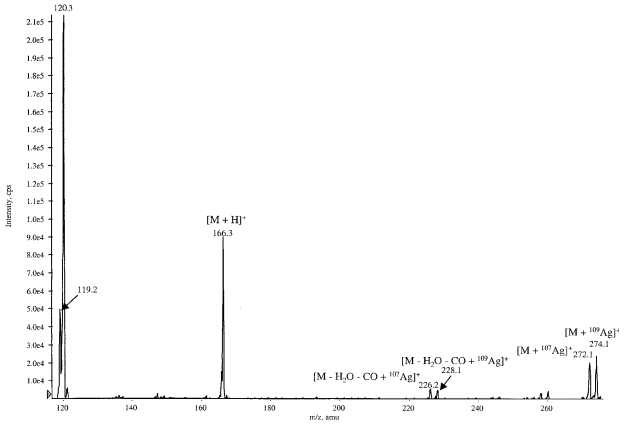

References

1. Bouchonnet, S.; Hoppilliard, Y.; Ohanessian, G. *J. Mass Spectrom.* **1995,** *30,* 172.
2. Gatlin, C. L.; Turecek, F. *J. Mass Spectrom.* **1995,** *30,* 1605.
3. Seto, C.; Stone, J. A. *Int. J. Mass. Spectrom.* **1999,** *192,* 289.
4. Hu, P.; Gross, M. L. *J. Am. Chem. Soc.* **1993,** *115,* 8821.
5. Hu, P.; Gross, M. L. *J. Am. Chem. Soc.* **1992,** *114,* 9153.
6. Cerda, B. A.; Cronett, L.; Wesdemiotis, C. *Int. J. Mass Spectrom.* **1999,** *193,* 205.
7. Brown, R. S.; Feng, J.; Reiber, D. C. *Int. J. Mass Spectrom.* **1997,** *169,* 1.
8. Fenn, J. B.; Mann, M.; Meng, C. K.; Wong, S. F.; Whitehouse, C. M. *Mass Spectrom. Rev.* **1990,** *9,* 37.
9. Lau, T.-C.; Wang, J.; Siu, K. W. M.; Guevrement, R. *J. Chem. Soc. Chem. Commun.* **1994**, 1487.
10. Cheng, Z. L.; Siu, K. W. M.; Guevrement, R.; Berman, S. *J. Am. Soc. Mass Spectrom.* **1992,** *3,* 281.
11. Cheng, Z. L.; Siu, K. W. M.; Guevrement, R.; Berman, S. *Org. Mass Spectrom.* **1992,** *27,* 1370.
12. Wilson, S. R.; Yasmin, A.; Wu, Y. *J. Org. Chem.* **1992,** *57,* 6941.
13. Blades, A. T.; Jayaweera, P.; Ikonomonu, M. G.; Kebarle, P. *Int. J. Mass Spectrom. Ion Processes* **1990,** *101,* 325.
14. Blades, A. T.; Jayaweera, P.; Ikonomonu, M. G.; Kebarle, P. *Int. J. Mass Spectrom. Ion Processes* **1990,** *102,* 251.
15. Blades, A. T.; Jayaweera, P.; Ikonomonu, M. G.; Kebarle, P. *J. Chem. Phys.* **1990,** *92,* 5900.
16. Shoeib, T.; Milburn, R. K.; Koyanagi, G. K.; Lavrov, V. V.; Bohme, D. K.; Siu, K. W. M.; Hopkinson, A. C. *Int. J. Mass Spectrom.* **2000,** *201,* 87.
17. Shoeib, T.; Hopkinson, A. C.; Siu, K. W. M. *J. Phys. Chem. B* **2001,** *105,* 12399.
18. Shoeib, T.; Siu, K. W. M.; Hopkinson, A. C. *J. Phys. Chem. A*, in press.
19. Chu, I. K.; Shoeib, T.; Guo, X.; Rodriquez, C. F.; Lau, T. C.; Hopkinson, A. C.; Siu, K. W. M. *J. Am. Soc. Mass Spectrom.* **2001,** *12,* 163.
20. El-Nahas, A. M.; Tajina, N.; Hirao, K. *J. Mol. Struct. (THEOCHEM)* **1999,** *469,* 201.
21. Shoeib, T.; Rodriquez, C. F.; Siu, K. W. M.; Hopkinson, A. C. *Phys. Chem.* **2001,** *3,* 853.
22. Frisch, M. J.; Trucks, G. W.; Schlegel, H. B.; Scuseria, G. E.; Robb, M. A.; Cheeseman, J. R.; Zakrzewski, V. G.; Montgomery, J. A., Jr.; Stratmann, R. E.; Burant, J. C.; Dapprich, S.; Millam, J. M.; Daniels, A. D.; Rudin, K. N.; Strain, M. C.; Farkas, O.; Tomasi, J.; Barone, V.; Cossi, M.; Cammi, R.; Mennucci, B.; Pomelli, C.; Adamo, C.; Clifford, S.; Ochterski, J.; Petersson, G. A.; Ayala, P. Y.; Cui, Q.; Morokuma, K.; Malick, D. K.; Rabuck, A. D.; Raghavachari, K.; Foresman, J. B.;

Cioslowski, J.; Ortiz, J. V.; Stefanov, B. B.; Liu, G.; Liashenko, A.; Piskorz, P.; Komaromi, I.; Gomperts, R.; Martin, R. L.; Fox, D. J.; Keith, T.; Al-Laham, M. A.; Peng, C. Y.; Nanayakkara, A.; Gonzalez, C.; Challacombe, M.; Gill, P. M. W.; Johnson, B.; Chen, W.; Wong, M. W.; Andres, J. L.; Head-Gordon, M.; Replogle, E. S.; Pople, J. A. *Gaussian 98, Revision A.5.* Gaussian Inc: Pittsburgh, PA, 1998.
23. Hohenberg, P.; Kohn, W. *Phys. Rev. B* **1964,** *136,* 864.
24. Kohn, W.; Sham, J. *Phys. Rev. A* **1965,** *140,* 1133.
25. Becke, A. D. *J. Chem. Phys.* **1992,** *97,* 9173.
26. Becke, A. D. *J. Chem. Phys.* **1992,** *96,* 2155.
27. Becke, A. D. *J. Chem. Phys.* **1993,** *98,* 5648.
28. Lee, C.; Yang, W.; Parr, R. G. *Phys. Rev. B* **1988,** *37,* 785.
29. Godbout, N.; Salahub, D. R.; Andzelm, J.; Wimmer, E. *Can. J. Chem.* **1992,** *70,* 560.
30. Godbout, N. *Ensemble de base pour la théorie de la fonctionnelle de la densité-Structures moléculaires, propriétés mono-électroniques et modèles de zéolites;* Ph.D. Thesis, University of Montreal, 1996.
31. Shoeib, T.; El Aribi, H.; Siu, K. W. M.; Hopkinson, A. C. *J. Phys. Chem. A* **2001,** *105,* 710.
32. El Aribi, H.; Shoeib, T.; Ling, Y.; Rodriquez, C. F.; Hopkinson, A. C.; Siu, K. W. M. *J. Phys. Chem. A,* in press.
33. Lee, V. W. M.; Li, H. B.; Lau, T. C.; Guevremont, R.; Siu, K. W. M. . *J. Am. Soc. Mass Spectrom.* **1998,** *9(8),* 760.
34. Grewal, R. N.; Rodriquez, C. F.; Shoeib, T.; Chu, I. K.; Tu, Y.-P.; Hopkinson, A. C.; Siu, K. W. M. *Eur. Mass Spectrom.* **2000,** *6,* 187.
35. Rogalewicz, F.; Hoppilliard, Y.; Ohanessian, G. *Int. J. Mass Spectrom.* **2000,** *195/196,* 565.
36. Dookernan, N. N.; Yalcin, T.; Harrison, A. G. *J. Mass Spectrom.* **1996,** *31,* 500.
37. Lei, Q. P.; Amster, I. J. . *J. Am. Soc. Mass Spectrom.* **1996,** *7(8),* 722.
38. Yalcin, T.; Wang, J.; Wen, D.; Harrison, A. G. . *J. Am. Soc. Mass Spectrom.* **1997,** *8(7),* 749.
39. Hoppilliard, Y.; Rogalewicz, F.; Ohanessian, G. . *Int. J. Mass Spectrom.* **2001,** *204(1–3),* 267.
40. Wen, D.; Yalcin, T.; Harrison, A. G. *Rapid Commun. Mass Spectrom.* **1995,** *9,* 1155.
41. Talaty, E. R.; Perera, B. A.; Gallardo, A. L.; Barr, J. M.; Van Stipdonk, M. J. *J. Phys. Chem. A* **2001,** *105,* 8059.
42. Smith, B. J.; Hall, N. E. *Chem. Phys. Lett.* **1997,** *279,* 165.
43. Beranova, S.; Cai, J.; Wesdemiotis, C. *J. Am. Chem. Soc.* **1995,** *117,* 9492.
44. Shoeib, T.; Hopkinson, A. C.; Siu, K. W. M. *J. Phys. Chem. A,* in press.
45. Chen, Y.-M.; Armentrout, P. B. *J. Phys. Chem.* **1995,** *99,* 11424.
46. Perera, B. A.; Ince, M. P.; Talaty, E. R.; Van Stipdonk, M. *J. Rapid Commun. Mass Spectrom.* **2001,** *15,* 615.
47. Lavant, H.; Hoppilliard, Y. *J. Mass Spectrom.* **1997,** *32,* 1037.